Розглянуто валідацію дистанційних колориметрических вимірювань на основі керованих рідкокристалічних фільтрів. Локальний синхронний наземний вимір в інфрачервоному і видимому діапазонах спектру і методика корекції їх даних підвищує оперативність визначення локальних витоків в магістральних трубопроводах. Методика дешифрування даних інфрачервоних вимірювань даних умовна і реальні кольори RGB вимірювання підвищують достовірність прийнятих рішень моніторингу

Ключові слова: екологічний моніторинг, синхронні вимірювання, інфрачервоний і видимий діапазон, достовірність, візуалізація

Рассмотрена валидация дистанционных колориметрических измерений на основе управляемых жидкокристаллических фильтров. Локальное синхронное наземное измерение в инфракрасном и видимом диапазонах спектра и методика коррекции их данных повышает оперативность определения локальных утечек в магистральных трубопроводах. Методика дешифрации данных инфракрасных измерений данными условных и реальных цветов RGB измерений повышает достоверность принятых решений мониторинга

Ключевые слова: экологический мониторинг, синхронные измерения, инфракрасный и видимый диапазон, достоверность, визуализация

UDC 681.325.5.181.4:528.8
DOI: 10.15587/1729-4061.2017.111220

VALIDATION OF AN INTEGRATED CONTROL SYSTEM WITH IMPROVEMENT IN EFFICIENCY AND RELIABILITY OF THE DECISIONS MADE FOR MONITORING

L. Bekirova
Doctor of Technical Sciences,
Associate Professor
Department of
Instrument-Making Engineering
Azerbaijan State Oil and Industrial University
Azadlyg ave., 20, Baku, Azerbaijan, AZ1010
E-mail: lala_bekirova@mail.ru

1. Introduction

One of the important aspects of remote sensing is monitoring the state of the environment, which is strongly affected by both the oil and gas industry at every stage of the production process. The task of operational ecological monitoring is aimed at accurate and early detection of contaminants in the products of industrial manufacturing, as well as determining places of their leaks. The information obtained by modern methods and tools makes it possible to quickly assess the state of the environment for timely action to prevent potentially dangerous consequences [1, 2].

Therefore, in order to improve reliability of control over the concentrations of substances that pollute the environment, it must be comprehensive and meet the requirements of their operation under specific conditions. Thus, completeness of the environmental database is the basic prerequisite for creating the most effective control-measuring systems (CMS) to control pollution of the environment.

Thus, development of new methods and techniques of measurement and their algorithmic-structural implementation implying comprehensive solution of the problems on improving the accuracy of color reproduction, informativeness, reliability and expansion of functionality of the systems for monitoring the environment, is a relevant task.

2. Literature review and problem statement

Of particular importance in environmental monitoring are the multilevel measurements, both in the narrow and expanded working range. Many modern systems of remote sensing (RS) of the Earth perform measurements in the visible, red and near infrared and parts of the spectrum. In [3], authors focus on obtaining values in the visible range and comparing RGB of measurements with the parameters of water quality for monitoring water surfaces. In [4], data validation of remote measurements in multilevel systems is presented in the form of the generalized character of the principle of validation of two-level measurements. Paper [5] describes a system with an extended working range, however, it considers only structural-technical solutions for distance measurement in the visible and near IR spectral bands. The possibility to register radiation in hundreds of very narrow spectral bands predetermines the use of integrated data obtained from hyperspectral sensors in cosmic space, airborne and ground-based (ALOS-3 (Japan), HyspIRI (USA), EnMap (Germany), PRISMA (Italy), Resurs-P No.1 (Russia)), presented in article [6]. In this case, non-informativeness of some ranges, leading to an increase in the amount of redundant information, often entails an unjustified complication of the systems' structure. In paper [7], authors proposed multilevel measurements using a hyperspectral instrument that has a panchromatic channel, RGB channels, and a channel

of near IR range. However, these devices carry out measurement with large quantities of channels (typically more than 100). It should be noted that an increase in the number of channels makes it possible to receive a large amount of information on the investigated object. Article [8] deals with issues related to the use of the sensor performing the role of optical and thermal sensor. It should be noted that it describes the role and purpose of this sensor while its physical implementation is not considered.

Paper [9] also provides information about acquiring large amounts of data by using hyperspectrometers. However, complexity of the visual decoding of that information makes it difficult to obtain all the information from the hypercube of data. That is why automatic data processing, as well as deriving useful information, requires new approaches related to the application of specific methods and data processing algorithms.

In order to provide high spatial resolution and geometrical accuracy in the RGB measurements, it is expedient to conduct them synchronously with ground-based radiometric and panchromatic measurements. Results of these measurements play an important role in the categorization of investigated objects [10]. However, the given paper considers expedience of conducting RGB remote measurements synchronized only with panchromatic measurements.

In [11], authors examined possibilities of improving informativeness of images during remote sensing by optimizing a process of merging the color (RGB) and panchromatic images and through a proper selection of functional dependence between the values of signals from these channels. They also consider a possibility of simultaneously conducting the RGB remote measurements using panchromatic measurements only.

Given the large areas covered with theproducts of oil and gas industry, it is necessary, when distributing local monitoring points, to take into account special features of production processes, characteristic for a prticular region, and to choose appropriate technical means.

This makes it possible to take necessary decisions timely and to predict the long-term status of the area. In order to comprehensively solve the task of monitoring, the system's structure should include ground-based (distributed on the ground), airborne and autonomous local control-measuring systems (LCMS). It is necessary, in this case, to model various complex processes occurring in the environment, so that the designed system meets metrological, operational and environmental requirements.

3. The aim and objectives of the study

The aim of present work is to improve reliability of the remote RGB measurements, to optimize operation time needed to detect local leaks in the main pipelines during monitoring.

To achieve the set aim, the following tasks had to be solved:

– to provide high spatial resolution and geometrical accuracy in the RGB measurements;

– to validate data derived from remote measurements;

– to enable automated control over production processes and to assess ecological status of the appropriate sites.

4. Structural model and principle of operation of the system with synchronous ground-based measurements

4. 1. Structural model of the control-measuring system

A set of airborne technical equipment, in contrast to that based on the gound, includes an optical receiving unit for the RGB and IR ranges, a unit of converters and normalization (UCN), a unit of additional parameters (UAP) and a databank (DB). The airborne LCMS makes it possible to remotely control the processes (for example, leakage of products) using the RGB and IR ranges of the spectrum. In this case, in order to assess ecological status of the ground-based facilities, the main measured parameters are spectral brightness coefficient, colorimetric data, and special radiation intensities.

Fig. 1 shows structural model of a multi-level control-measuring system designed to control the process of oil transportation and oil leaks.

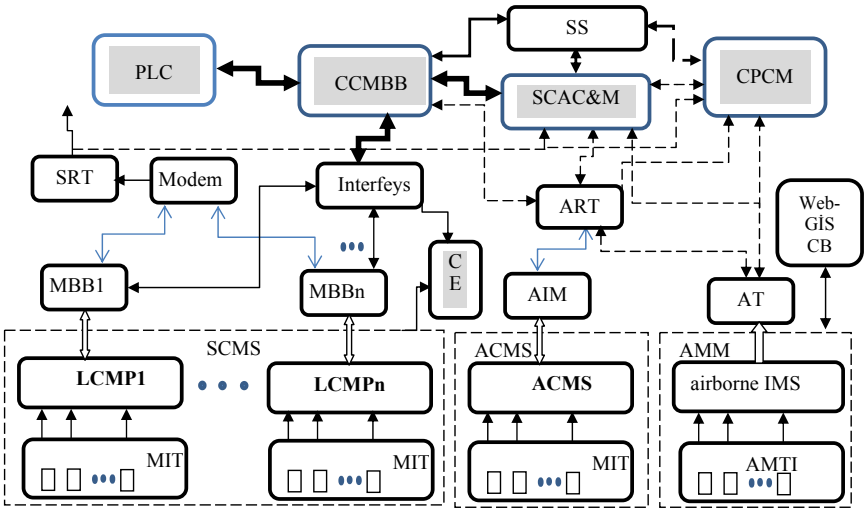

Fig. 1. Block diagram of a multilevel control-measuring system

The following designations are used in Fig. 1. LCMP – local control-measuring point, MIT – measuring instruments and transducers, SCMS – sectoral control- measuring system, ACMS – autonomous control-measuring system, ACMP – autonomous control-measuring point, AMTI – airborne measuring transducers and instruments, airborne IMS – airborne information measuring system, AMM – airborne measuring module, AT – airborne transceiver, AIM – autonomous interface module, IMIO-interface module of input-output, CE – controlling elements, SRT – system of reception and transmission, I– interface, M – modem, ART – autonomous receiver-transmitter, CPCM – central point of control and management, SCAC&M – sectoral central automated control and management, NCMIO – network

connecting module of input-output, PLC – PLC system, SS – SCADA system.

Equipment of the ground-based LCMP includes: sensors of technological process (such as pressure sensors (PS), temperature sensors (TS), flow rate sensors (FRS), viscosity sensors) and additional sensors (such as spectrometer, colorimeter and IR radiometer, direction sensors and wind speed sensors, gas analyzers, hygrometers, dynamic sensors that register technogenic or seismic vibrations, etc.). The following units are used for data processing and information exchange: local computing module – LCM (microcontroller module); unit of registration and 2D-3D indication; memory unit (MU); sound and light alarm unit (SLAU); manual control unit (MCU); coordinate-connecting block to WEB/GIS (CCB); transmission and reception unit (TRU); software unit (SU).

Depending on the conditions of location of LCMS, the methods and means of communication are selected (CAN, radio, USB, fiber optic cable). In this case, satellite positioning systems (GPS) are widely used. Access to various sources of information is provided using Web-GIS services that bring technologies of remote sensing to the new, higher level, expanding thereby the scope of their application.

4. 2. Principle of research into a two-level system by the RGB (PAN) and IR ranges between two LCMS of monitoring

Monitoring of the pathway of main pipelines using manned and unmanned carriers, from technical and economic points of view, is more appropriate, despite the high resolution capability of space systems for remote sensing. When transporting oil by pipelines, specific environmental peculiarities of the area are taken into account, special features of the pipeline, a need for technical diagnosis, potential leakage volumes, as well as the results of analysis of environmental sensitivity and risks.

Modeling the remote and contact control over processes, as well control of leakage in order to prevent it, makes it possible to reduce the effect of oil spills to the environment. In this case, the technique, algorithm and software designed for monitoring and diagnosis of the main pipelines enable prediction of change in the state of the environment, local leakage diagnosis and timely forecasting of operating modes.

For this purpose, the airborne LCMS of the complex employs a remote system working in the RGB and IR bands (Fig. 2).

For remote registration of the reflected light flux and thermal radiation, which characterize the examined object in conditionally selected four points of measuring that are aligned with material points of the area, three RGB and two IR liquid-crystal-based filters are applied.

Results of the interrelated measurements by the RGB and infrared (IR) channels are given in Table 1.

Between two LCMS, located over the examined pipeline, a set of n measurements is collected, where n is determined by the step of temporal discretization and by the length of the section between the two LCMS. In this case, conditionally in $1 \div n$ points, remote measurements ($D1$, $D2$, $D3$ ... Dn) and ground-based ($N1$,..., Nm) measurements are implied.

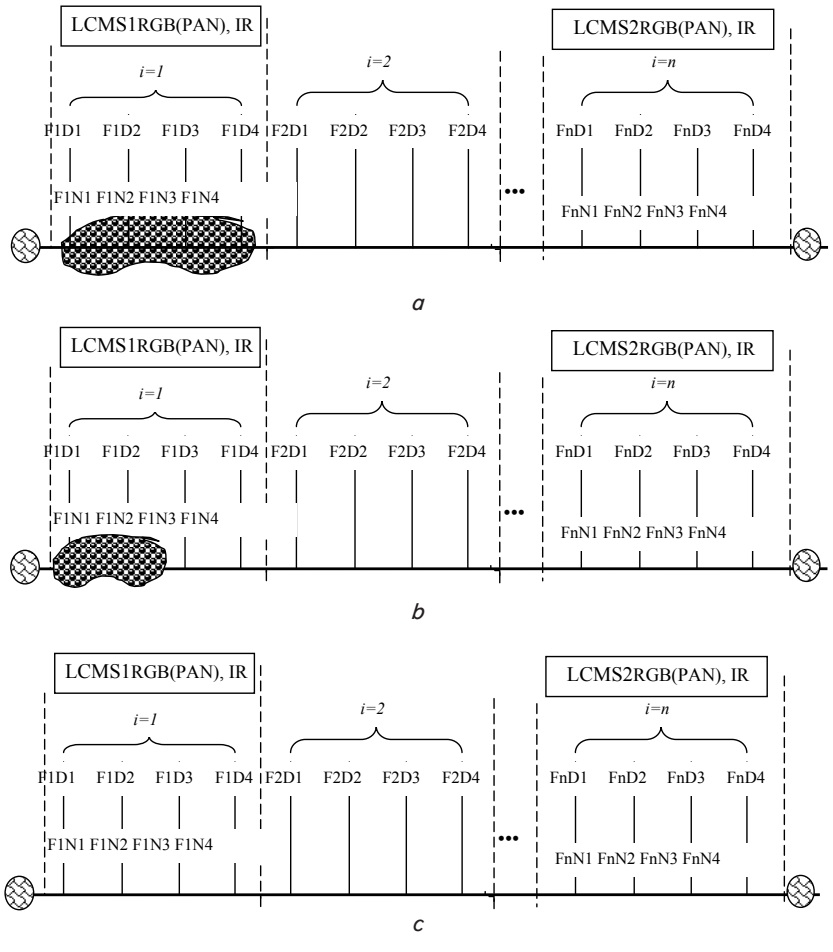

Fig. 2. Distribution of two-level measurements by RGB (PAN) and IR ranges between two LCMS in accordance with the state of the plot: *a* – completely polluted, k=1; *b* – partly polluted, k=2; *c* – not polluted, k=3

Table 1

Distribution of measuring results by the RGB and IR channels

Set of measurements $i=1\div n, j=1\div 4$		Measurement results	
		By the RGB channels	By the IR channels
i=1 (LCMS 1)	i_1	$F_{1d1}(RGB)=f_1(L_{RD1}, L_{GD1}, L_{BD1})$	$F_{1d1}(\dot{I}Q)=f_1(\dot{I}_{IQ1D1}, \dot{I}_{IQ2D1})$
		$F_{1N1}(RGB)=f_1(L_{RN1}, L_{GN1}, L_{BN1})$	$F_{1N1}(\dot{I}Q)=f_1(\dot{I}_{IQ1N1}, L_{IQ2N1})$
	i_2	$F_{1d2}(RGB)=f_1(L_{RD2}, L_{GD2}, L_{BD2})$	$F_{1d2}(IQ)=f_1(I_{IQ1D2}, I_{IQ2D2})$
		$F_{1N2}(RGB)=f_1(L_{RN2}, L_{GN2}, L_{BN2})$	$F_{1N2}(\dot{I}Q)=f_1(\dot{I}_{IQ1N2}, L_{IQ2N2})$
	i_3	$F_{1d3}(RGB)=f_1(L_{RD3}, L_{GD3}, L_{BD3})$	$F_{1d3}(IQ)=f_1(I_{IQ1D3},I_{IQ2D3})$
		$F_{1N3}(RGB)=f_1(L_{RN3}, L_{GN3}, L_{BN3})$	$F_{1N3}(\dot{I}Q)=f_1(\dot{I}_{IQ1N3}, L_{IQ2N3})$
	i_4	$F_{1d4}(RGB)=f_1(L_{RD4}, L_{GD4}, L_{BD4})$	$F_{1d4}(IQ)=f_1(I_{IQ1D4}, L_{IQ2D4})$
		$F_{1N4}(RGB)=f_1(L_{RN4}, L_{GN4}, L_{BN4})$	$F_{1N4}(IQ)=f_1(I_{IQ1N4}, I_{IQ2N4})$
i=2 intermediate	i_1	$F_{2d1}(RGB)=f_2(L_{RD1}, L_{GD1}, L_{BD1})$	$F_{2d1}(\dot{I}Q)=f_2(\dot{I}_{IQ1D1}, \dot{I}_{IQ2D1})$
	i_2	$F_{2d2}(RGB)=f_2(L_{RD2}, L_{GD2}, L_{BD2})$	$F_{2d2}(IQ)=f_2(I_{IQ1D2}, I_{IQ2D2})$
	i_3	$F_{2d3}(RGB)=f_2(L_{RD3}, L_{GD3}, L_{BD3})$	$F_{2d3}(IQ)=f_2(I_{IQ1D3},I_{IQ2D3})$
	i_4	$F_{2d4}(RGB)=f_2(L_{RD4}, L_{GD4}, L_{BD4})$	$F_{2d4}(IQ)=f_2(I_{IQ1D4}, L_{IQ2D4})$
...		...	...
$i=n-1$ intermediate	i_1	$F_{n\text{-}1d1}(RGB)=f_{n\text{-}1}(L_{RD1}, L_{GD1}, L_{BD1})$	$F_{n\text{-}1d1}(\dot{I}Q)=f_{n\text{-}1}(\dot{I}_{IQ1D1}, \dot{I}_{IQ2D1})$
	i_2	$F_{n\text{-}1d2}(RGB)=f_{n\text{-}1}(L_{RD2}, L_{GD2}, L_{BD2})$	$F_{n\text{-}1d2}(IQ)=f_{n\text{-}1}(I_{IQ1D2}, I_{IQ2D2})$
	i_3	$F_{n\text{-}1d3}(RGB)=f_{n\text{-}1}(L_{RD3}, L_{GD3}, L_{BD3})$	$F_{n\text{-}1d3}(IQ)=f_{n\text{-}1}(I_{IQ1D3},I_{IQ2D3})$
	i_4	$F_{n\text{-}1d4}(RGB)=f_{n\text{-}1}(L_{RD4}, L_{GD4}, L_{BD4})$	$F_{n\text{-}1d4}(IQ)=f_{n\text{-}1}(I_{IQ1D4}, L_{IQ2D4})$
$i=n$ (LCMS 2)	i_1	$F_{nd1}(RGB)=f_n(L_{RD1}, L_{GD1}, L_{BD1})$	$F_{nd1}(\dot{I}Q)=f_n(\dot{I}_{IQ1D1}, \dot{I}_{IQ2D1})$
		$F_{nN1}(RGB)=f_n(L_{RN1}, L_{GN1}, L_{BN1})$	$F_{nN1}(\dot{I}Q)=f_n(\dot{I}_{IQ1N1}, L_{IQ2N1})$
	i_2	$F_{nd2}(RGB)=f_n(L_{RD2}, L_{GD2}, L_{BD2})$	$F_{nd2}(IQ)=f_n(I_{IQ1D2}, I_{IQ2D2})$
		$F_{nN2}(RGB)=f_n(L_{RN2}, L_{GN2}, L_{BN2})$	$F_{nN2}(\dot{I}Q)=f_n(\dot{I}_{IQ1N2}, L_{IQ2N2})$
	i_3	$F_{nd3}(RGB)=f_n(L_{RD3}, L_{GD3}, L_{BD3})$	$F_{nd3}(IQ)=f_n(I_{IQ1D3},I_{IQ2D3})$
		$F_{nN3}(RGB)=f_n(L_{RN3}, L_{GN3}, L_{BN3})$	$F_{nN3}(\dot{I}Q)=f_n(\dot{I}_{IQ1N3}, L_{IQ2N3})$
	i_4	$F_{nd4}(RGB)=f_n(L_{RD4}, L_{GD4}, L_{BD4})$	$F_{nd4}(IQ)=f_n(I_{IQ1D4}, L_{IQ2D4})$
		$F_{nN4}(RGB)=f_n(L_{RN4}, L_{GN4}, L_{BN4})$	$F_{nN4}(\dot{I}Q)=f_n(\dot{I}_{IQ1N4}, L_{IQ2N4})$

As can be seen from Fig. 2, at i=1 and $i=n$ remote sensing and ground-based measurements are carried out synchronously; in the remaining moments – asynchronously (due to the lack of ground-based measurements).

5. Validation of data obtained by the ground-based measurements. Results of the research

Distribution of results of measurements using the system (Fig. 2) for RGB and IR channels are given in Tables 2, 3. In this case, we observe distribution of the appropriate data in order, given in Table 1. The presented results of remote (Table 2) and ground-based (Table 3) measurements correspond to the areas nearby LCMS1, LCMS2 and intermediate plots. In Tables 2, 3, $F_{iz}D_j$ and $F_{iz}N_j$ (i=1÷4; j=1÷4 and k=1÷3) are the elements of the sample sets whose values are the averaged results of 10-fold measurements conducted by the RGB and infrared measurement tools. Here i is the number of samples corresponding to a set of conducted measurements; j is the number of measurements performed at one plot, k is the number of state of each plot. For example, k=1 corresponds to fully polluted, k=2 – to partly polluted, and k=3 – to unpolluted states. To simplify the process of measuring, LCMS1 and LCMS2 are accepted to be located at a short distance.

To reduce spatial bias for data that correspond to the RGB colors, a one-time PAN measurement is implied [13].

When performing synchronous measurements, the root mean square of a representation error for, respectively, the RGB and IR channels for 1 and n-th sets of measurements is determined as follows:

– for the 1-st set of RGB measurements:

$$\overline{\varepsilon_{1RGB11}{}^2}=\overline{\left[\mathrm{F}_{1D1}(RGB)-F_{1N1}(RGB)\right]^2},$$

$$\overline{\varepsilon_{1RGB2}{}^2}=\overline{\left[F_{1D2}(RGB)-F_{1N2}(RGB)\right]^2}, \quad (1)$$

$$\overline{\varepsilon_{1RGB3}{}^2}=\overline{\left[F_{1D3}(RGB)-F_{1N3}(RGB)\right]^2},$$

$$\overline{\varepsilon_{1RGB4}{}^2}=\overline{\left[F_{1D4}(RGB)-F_{1N4}(RGB)\right]^2};$$

– for the 1-st set of IR measurements:

$$\overline{\varepsilon_{1IR1}{}^2}=\overline{\left[\mathrm{F}_{1D1}(IR)-F_{1N1}(IR)\right]^2},$$

$$\overline{\varepsilon_{1RGB2}{}^2}=\overline{\left[\mathrm{F}_{1D2}(IR)-F_{1N2}(IR)\right]^2}, \quad (2)$$

$$\overline{\varepsilon_{1IR3}{}^2}=\overline{\left[\mathrm{F}_{1D3}(IR)-F_{1N3}(IR)\right]^2},$$

$$\overline{\varepsilon_{1IR4}{}^2}=\overline{\left[\mathrm{F}_{1D4}(IR)-F_{1N4}(RGB)\right]^2}.$$

Table 2

Distribution of results of remote measurements using the system for the RGB and IR channels

No. state	$F1_kDj$; (j=1–4, k=1–3)				m_{F1D1k}	$F2_kDj$; (j=1–4, k=1–3)				m_{F2D1k}	$F3_kDj$; (j=1–4, k=1–3)				m_{F3D1k}	$F4_kDj$; (j=1–4, k=1–3)				m_{F4D1k}
	j=1	j=2	j=3	j=4		j=1	j=2	j=3	j=4		j=1	j=2	j=3	j=4		j=1	j=2	j=3	j=4	
k=1	12	14	14	13	13.3	6	7	7	7	6.75	7.3	7.35	7.40	7.2	7.31	6.23	7.45	7.42	7.27	7.09
k=2	14	14	7	7	10.5	7	7	6	6	6.50	6.2	7.40	6.52	6.4	6.63	7.31	7.37	6.60	6.46	6.94
k=3	6.15	7	7	7	6.79	7	7	7	6	6.75	7.0	7.26	7.32	6.3	6.97	7.35	7.35	7.40	6.45	7.14

Table 3

Distribution of results of the ground-based measurements using the system for the RGB and IR channels

No. state	$F1kNj$; (j=1–4, k=1–3)				m_{F1N1k}	$F2_kDj$; (j=1–4, k=1–3)				m_{F2D1k}	$F3_kDj$; (j=1–4, k=1–3)				m_{F3D1k}	$F4_kNj$; (j=1–4, k=1–3)				m_{F4N1k}
	j=1	j=2	j=3	j=4		j=1	j=2	j=3	j=4		j=1	j=2	j=3	j=4		j=1	j=2	j=3	j=4	
k=1	13	15.1	15.05	14	14.9	6	7	7	7	6.75	7.3	7.35	7.4	7.2	7.31	7.2	8.35	8.3	8.2	8.01
k=2	15.25	15	8.2	8	11.1	7	7	6	6	6.50	6.2	7.4	6.52	6.4	6.63	8.3	8.46	7.52	7.4	7.92
k=3	7	8	8	7.45	7.61	7	7	7	6	6.75	7	7.26	7.32	6.3	6.97	8	8.26	8.22	7.23	7.93

Given that

$$\varepsilon_{RGB}{}^2 = 2\sigma_s^2\left[1-r_{RGB}\right] \text{ and } \varepsilon_{IR}{}^2 = 2\sigma_s^2\left[1-r_{IR}\right],$$

where σ_s is the root mean square deviation of the signal, which is equal to:

$$\sigma_{sRGB} = \sqrt{\frac{1}{4}\sum_1^4 (F_{RGBDi} - \overline{F}_{RGBD})^2},$$

$$\sigma_{sIR} = \sqrt{\frac{1}{4}\sum_1^4 (F_{IRDi} - \overline{F}_{IRD})^2}. \quad (3)$$

r_{RGB} and r_{IR} linear coefficient of inter-element correlation in rows in this case is:

$$r_{RGB} = \frac{\sum (D_{RGBi} - \overline{D}_{RGB})\cdot(N_{RGBi} - \overline{N}_{RGB})}{\sqrt{\sum (D_{RGBi} - \overline{D}_{RGB})^2 \cdot \sum (N_{RGBi} - \overline{N}_{RGB})^2}},$$

$$r_{IR} = \frac{\sum (D_{IRi} - \overline{D}_{IR})\cdot(N_{IRi} - \overline{N}_{IR})}{\sqrt{\sum (D_{IRi} - \overline{D}_{IR})^2 \cdot \sum (N_{IRi} - \overline{N}_{IR})^2}}. \quad (4)$$

Fig. 2 shows that the remaining sets include results only of remote measurements (in the RGB (IR) channels) that are determined by the appropriate step of discretization and cover perticular areas.

Control and diagnosis of the main pipelines make it possible to predict a change in the state of the environment, to diagnose local leakages and to forecast operational modes on time.

To implement this possibility, there are three tasks that have to be solved.

At present, within a framework of monitoring programmes, in addition to the traditional "manual" probing of the object of research, emphasis is on data collection using electronic measuring devices for remote monitoring in real time. In this regard, the first task is to validate remote measurements against the ground-based measurements in such a way so that their results with a certain error compensate for the absence of ground-based measurements.

The remote measurements conducted make it possible to assess condition of the examined object and to monitor dynamics of this state in time and space, which allows successful solution to many important practical tasks in the case when, for one reason or another, it is not possible or impractical to conduct the ground-based measurements.

The advantage of remote monitoring is that one base station can exploit many channels of measurements for data storage and analysis. This significantly improves monitoring efficiency when the threshold levels of controlled indocators are reached. Such an approach makes it possible to perform swift action based on data from monitoring if the threshold level is exceeded. This raises the question: under what conditions can the ground-based measurements be replaced with the remote measurements?

We shall consider a sample of remote (F_{iDi}(RGB), F_{iDi}(IR)) and (F_{iNi}(RGB), F_{iNi}(IR)) ground-based measurements, the sets of which are denoted, respectively, through {D} and {N}:

$$\{D\} = \left\{D_i^j : F_{iDj}(FGB) \cup F_{iDj}(IR);\ i=\overline{1,n},\ j=\overline{1,4}\right\}, \quad (5)$$

$$\{N\} = \left\{N_i^j : F_{iNj}(FGB) \cup F_{iNj}(IR);\ i=n, i=n\ j=\overline{1,4}\right\}.$$

It is required to find such characteristic functions along the D_i and N_i coordinates so that the following condition is satisfied:

$$F(D_i, N_i) = \begin{cases} 1, \text{ if } \{D_i\} \equiv \{N_i\}, \\ 0, \text{ if } \{D_i\} \neq \{N_i\}. \end{cases} \quad (6)$$

Here "≡" denotes equality of statistical parameters.

We shall formulate a mathematical statement of the problem.

There are two samples, $\{D_i\}$ and $\{N_i\}$, each of which consists of m and n measurements, respectively. It is required to determine statistical equalities of these samples. Note that in the proposed case the measurements were carried out under the same conditions and with the same measurement tools, which is why we shall assume that the general totalities of the ground-based and remote measurements comply with a normal distribution law.

Samples from the first set of measurements of these general totalities will be denoted as follows:

$$D_i^j = \left(D_i^1, D_i^2, \ldots, D_i^n\right),$$

$$N_i^j = \left(N_i^1, N_i^2, \ldots, N_i^m\right), \quad (7)$$

where i defines the number of the current set of measurements, j determines the number of repeated results of the remote (j=1, n) and ground-based (j=1, m) measurements at the i-th set of measurements.

Assume that for the above general totalities average values are known, $\overline{D}$ and $\overline{N}$, but their root-mean-square deviations σ_D^2 and σ_N^2 are unknown. It is required to verify a hypothesis on the equality of averages of two totalities given the known sample variations $\overline{\sigma}_D^2$ and $\overline{\sigma}_N^2$.

For this purpose, we shall use the following criterion:

$$t_{\text{calculate}} = \frac{\overline{D} - \overline{N}}{\sqrt{\frac{(n-1)\sigma_D^2 + (m-1)\sigma_N^2}{n+m-2}}} \cdot \sqrt{\frac{nm}{n+m}}. \quad (8)$$

Hypothesis $\overline{D} \equiv \overline{N}$ is rejected if

$$\left|t_{\text{calculate}}\right| > t_\alpha(n+m-2),$$

where $t_\alpha(n+m-2)$ is the critical boundary of Student's distribution, corresponding to the level of significance. Assuming that the number of remote and ground-based measurements is n, formula (8) takes the following form:

$$t_{\text{calculate}} = \frac{\overline{D} - \overline{N}}{\sqrt{\frac{\overline{\sigma}_D^2 + \overline{\sigma}_N^2}{n}}}. \quad (9)$$

For accepting the hypothesis, the following conditions must be met:

$$\left|\overline{D} - \overline{N}\right| \le \sqrt{\frac{\overline{\sigma}_D^2 + \overline{\sigma}_N^2}{n}} \cdot t_\alpha\left(2(n-1)\right)$$

or

$$\frac{\left|\overline{D} - \overline{N}\right|}{\sqrt{\frac{\overline{\sigma}_D^2 + \overline{\sigma}_N^2}{n}}} < t_\alpha\left(2(n-1)\right). \quad (10)$$

The second task is to estimate the error of results of the remote measurements in the absence of results of the ground-based measurements. To solve this problem, assume that the sample variances $\overline{\sigma}_D^2$ and $\overline{\sigma}_N^2$ are connected by the following relations $\left\|\overline{\sigma}_D^2 - \overline{\sigma}_N^2\right\| = \varepsilon$ from (10).

Then find the deviation from ε:

$$\overline{\sigma}_D^2 = \overline{\sigma}_N^2 \pm \varepsilon, \quad (11)$$

where

$$\varepsilon = n\left[\frac{\overline{D} - \overline{N}}{t_\alpha\left(2(n-1)\right)}\right] - 2\overline{\sigma}_D^{-2}. \quad (12)$$

This means that, in order to ensure equality of averages of the results of remote and ground-based measurements, their root-mean-square deviations must be less than the values of ε, calculated from formula (12).

To solve the first of the above set problems (replacement of the ground-based measurements with remote measurements, validation and correction of their results with a certain error), we shall perform statistical processign of data given in Tables 2, 3.

To verify hypothesis (6) (on the proximity of results from the ground-based and remote measurements), we shall calculate $t_{\text{calculate}}$ (9).

Results of data processing from the ground-based and remote measurements are given in Table 4 and Fig. 3.

σ_{D1} and σ_{D4} (σ_{N1} and σ_{N4}) are the root-mean-square deviations of the sample corresponding to a dataset of the remote (ground-based) measurements for the tested plots (k=1, heavily polluted), (k=2, partially polluted), and (k=3, not polluted). σ_{1DNQ} and σ_{4DNQ} are the root-mean-square deviations of general totalities of data from the above measurements (Fig. 3, *a*, symbol σ is shown as *s*).

ν_{D1} and ν_{D4} (ν_{N1} and ν_{N4}) is the quadratic coefficient of sample variation, ν_{1DNQ} and ν_{4DNQ} is the quadratic coefficient of variation of the totality of data from the remote and ground-based measurements for k=1, k=2 and k=3 (Fig. 3, *b*, symbol ν is shown as *n*).

r_{1DN} and r_{4DN} is the coefficient of inter-element correlation in the lines of remote and ground-based measurements, α is the significance level, ε are the errors in the results of remote measurements. t_{ABS} is the absolute value of $t_{\text{calculate}}$ determined from (9) (Fig. 3, *c*, symbol ε is shown as e, symbol α as a).

In this case, collection and preliminary processing of the RGB and IR data is performed during measuring in the airborne part of the system, which shortens the time for additional data processing (typically carried out in a ground-based center) and makes it possible to provide the user with necessary information on time.

Table 4

Results of processing data from the ground-based and remote measurements

No. state	σ_{D1}	σ_{N1}	σ_{1DNQ}	σ_{D4}	σ_{N4}	σ_{4DNQ}	ν_{D1}	ν_{N1}	ν_{1DNQ}	ν_{D4}	ν_{N4}	ν_{4DNQ}	r_{1DN}	r_{4DN}	ε_{D1N1}	t_{ABS}	$t_\alpha(k)$ α=0,05 k=6	$t<ta\,(k)$ – othesis is true
k=1	0.96	1.0	0.99	0.58	0.55	0.67	0.07	0.07	0.07	0.08	0.07	0.09	1.0	1.0	0.001	1.48	2.45	
k=2	4.04	4.06	3.55	0.47	0.54	0.66	0.38	0.35	0.32	0.07	0.07	0.09	1.0	1.0	0.01	0.78	2.45	
k=3	0.43	0.48	0.57	0.46	0.48	0.57	0.06	0.06	0.08	0.06	0.06	0.08	0.84	0.97	0.10	1.73	2.45	

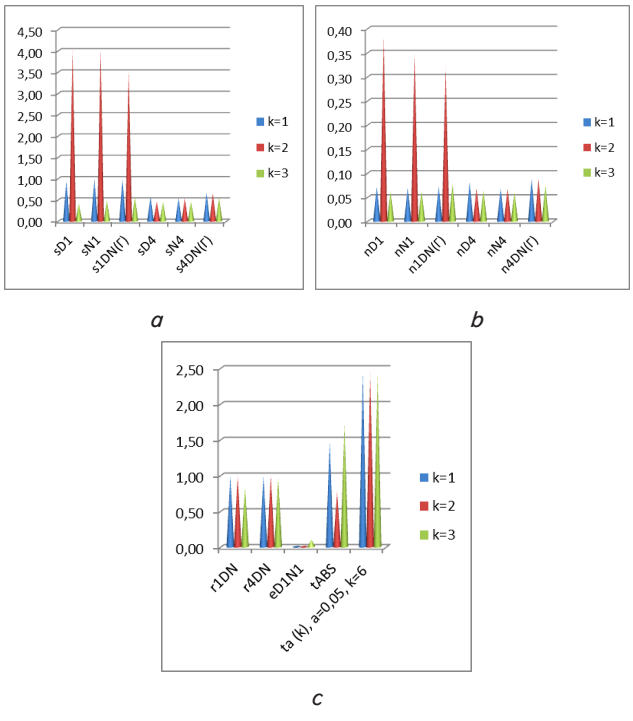

Fig. 3. Results of processing data from the ground-based and remote synchronous measurements: *a* — root-mean-square deviation of the sample and general totalities; *b* — squared coefficient of the sample variation and general totalities; *c* — coefficient of inter-element correlation of error in the remote data, as well as $t_{calculate}$ and t_{α}

Based on these results, it is possible to draw a conclusion on that the ground-based and remote measurements data satisfy conditions of hypothesis ($\overline{D} \equiv \overline{N}$), that is, the conditions $t_{\alpha} > |t_{calculate}|$ (2.45>1.48) (at k=6 and α=0.05) are fulfilled, and

$$\left|\overline{D}-\overline{N}\right| \le \sqrt{\frac{\overline{\sigma}_D^2+\overline{\sigma}_N^2}{n}} \cdot t_{\alpha}\left(2(n-1)\right).$$

6. Discussion of results of the multi-level measurements for the examined areas

Given the above, the conclusion follows that in the absence of the ground-based measurements, intermediate data from the remote measurements can be used instead (taking into account an error of (ε)).

We shall consider the third problem that comes down to predicting the location of territory, over which a leakage of oil occurred.

To determine a place of leakage and approximate size of the polluted sites, specialized algorithms can be employed for the set (1 and n) of results of the remote and ground-based measurements (*F1D*1, *F1D*2, *F1D*3 and *F1D*4) and (*F1N*1, *F1N*2, *F1N*3 and *F1N*4), related to LCMS1, and (*FnD*1, *FnD*2, *FnD*3 and *FnD*4) and (*FnN*1, *FnN*2, *FnN*3 and *FnN*4), associated with LCMS2, for the RGB (IR) channels.

Assume that there are certain sets of measurement results for uniform areas between two LCMS corresponding to a different condition of the certain areas of examined terrain:

a) all values from the first set correspond to the polluted site;

b) part of the values from the first set corresponds to the polluted site (place of leakage);

c) two adjacent sets correspond to the unpolluted sites.

In order to conduct the analysis, we shall apply hypothetical data from the remote (Table 2) and ground-based (Table 3) measurements.

When performing the IR measurements, a digital equivalent, corresponding to the polluted area, will be of increased importance due to the absorption of incident light.

If we conditionally accept that the results of measurements were obtained during IR measurement, then the data acquired can be distributed according to the degree of pollution in the following way:

1) if the first set matches a fully polluted site, while the second set corresponds to the unpolluted site, then the following conditions are to be tested:

$$\overline{F_1 D_1^4} >> \overline{F_2 D_1^4} \text{ and } \sigma_{s1} \approx \sigma_{s2}; \quad (13)$$

2) if the first set matches partially polluted sites, while the second set corresponds to the unpolluted site, then the following conditions are to be tested:

$$\overline{F_1 D_1^4} > \overline{F_2 D_1^4} \text{ and } \sigma_{s1} >> \sigma_{s2}; \quad (14)$$

3) if the first and the second sets match an unpolluted site, then, in contrast to the first and the second cases, the following conditions are to be tested:

$$\overline{F_1 D_1^4} \approx \overline{F_2 D_1^4} \text{ and } \sigma_{s1} \approx \sigma_{s2}. \quad (15)$$

To improve reliability of the obtained data on the correspondence of the polluted site to the measurement set, we carry out a pair-wise alignment of measuring results from neighbouring sets and then test conditions (13), (14) and (15) again.

For example, for the first case, we obtain, after a pair-wise alignment of the first and the second sets, the following sets: 12, 14, 6, 7, and 14, 13, 7, 7. Meeting the above-specified conditions confirms the determined location of the polluted site (a leakage zone).

Results of processing the ground-based and remote measurements (Tables 2, 3) allow us to locate the place of leakage.

In addition, simultaneous analysis with regard to the properties of RGB measurements (conditions similar to (13) to (15)) improves reliability of the results obtained. In this case, it is accepted that the data were derived from the corresponding plots of the examined area.

During visualization of the measurement results, obtained in the IR range (their decoding using conditional colors), and when comparing them with data obtained using actual colors in the RGB channels of the same object, there is the possibility to obtain reliable information and to take a correct decision for the categorization of objects. In this case, by the Wien's law, based on data obtained in the IR channels, high-intensity matches the color of the short wavelength of the visible range of the spectrum.

Thus, when diagnosing a polluted area, it is possible to use data from the synchronously conducted ground-based and remote measurements, as well as intermediate data from the remote measurements only, with regard to validation.

6. Conclusions

1. To improve spatial resolution and geometrical accuracy in the RGB measurements, it is proposed to use the IR and panchromatic measurements in combination, using controlled liquid crystal filters.

2. A technique is devised for the remote and locally synchronous ground-based measurements to validate and correct their results with a certain error. This technique makes it possible, in the case of impossibility or inadvisability of carrying out the ground-based measurements, to perform a rapid assessment of the condition of examined area based on the data from remote measurements with regard to validation.

3. A structure is developed of the automated system to control processes and assess ecological status of the appropriate terrain sites, which enables monitoring of the condition of examined area simultaneously with a control over key production processes in order to solve a problem comprehensively.

3. The IR data visualization is proposed (using conditional colors), as well as their comparison to the data of actual colors in the RGB measurements with a minimal number of channels based on liquid crystal filters to improve reliability of information and to take a correct decision in the categorization of objects.

References

1. Bushmeleva, K. I. The automation concept of ecological monitoring of environmental pollution in the Khanty-Mansi Autonomous Area [Text] / K. I. Bushmeleva, I. I. Plusnin, S. M. Sisoev, P. E. Bushmelev, A. V. Elnikov // Modern high technology. – 2007. – Issue 3. – P. 41–43.
2. Bulicheva, E. V. The results of satellite monitoring of oil pollution in South-Eastern Baltic for 2006–2009s. [Text] / E. V. Bulicheva, A. G. Kostyanoy // Modern problems of remote probing of the Earth from space. – 2011. – Vol. 8, Issue 2. – P. 74–83.
3. Goddijn-Murphy, L. Fundamentals of in Situ Digital Camera Methodology for Water Quality Monitoring of Coast and Ocean [Text] / L. Goddijn-Murphy, D. Dailloux, M. White, D. Bowers // Sensors. – 2009. – Vol. 9, Issue 7. – P. 5825–5843. doi: 10.3390/s90705825
4. Bekirova, L. R. Principle of validation of multilevel RGB colorimetric systems of remote sensing [Text] / L. R. Bekirova // Proceedings of the National Aviation University. – 2013. – Vol. 57, Issue 4. doi: 10.18372/2306-1472.57.5561
5. Bekirova, L. R. Modified Board System for Ecological Monitoring of Ground-Based Objects State [Text] / L. R. Bekirova // Advanced Materials Research. – 2012. – Vol. 508. – P. 275–279. doi: 10.4028/www.scientific.net/amr.508.275
6. D'Odorico, P. Monitoring the Spectral Performance of the APEX Imaging Spectrometer for Inter-Calibration of Satellite Missions. Vol. 63 [Text] / P. D'Odorico // Remote Sensing Series. – University of Zurich Switzerland, 2012. – 83 p.
7. Markelin, L. Validation of the radiometric processing chain of the leica ADS40 airborne photogrammetric sensor [Text] / L. Markelin, E. Honkavaara, U. Beisl, I. Korpela // ISPRS TC VII Symposium – 100 Years ISPRS. – 2010. –Vol. XXXVIII. – P. 145–149.
8. Vorovencii, I. Optical and thermal space-borne sensors – a review [Text] / I. Vorovencii // Bulletin of the Transilvania University of Bra ov. – 2010. – Vol. 3, Issue 52.
9. Wang, B. Spatial entropy based mutual information in hyperspectral band selection for supervised [Text] / B. Wang, X. Wang, Z. Chen // International Journal of Numerical Analysis and Modeling. – 2012. – Vol. 9, Issue 2. – P. 181–192.
10. Wang. J. Distinct image fusion methods for landslide information enhancement [Text] / J. Wang, J. X. Zhang, Z. J. Liu. – Institute of Photogrammetry & Remote Sensing, CASM, Beijing, 2004. – Available at: http://isprs-wgii-1.casm.ac.cn/source/DISTINCT%20IMAGE%20FUSION%20METHODS%20FOR%20LANDSLIDE%20INFORMATION%20ENHANCEMENT.pdf
11. Bekirova, L. R. Optimization problems of the color signals transformation while merging the satellite of black-and-white and color images [Text] / L. R. Bekirova // Information Technology. – 2013. – Issue 6. – P. 60–62.